

Determination of Critical Exponents from the Multifragmentation of Gold Nuclei

M. L. Gilkes,¹ S. Albergo,² F. Bieser,⁶ F. P. Brady,³ Z. Caccia,² D. A. Cebra,³ A. D. Chacon,⁷ J. L. Chance,³ Y. Choi,^{1,*} S. Costa,² J. B. Elliott,¹ J. A. Hauger,¹ A. S. Hirsch,¹ E. L. Hjort,¹ A. Insolia,² M. Justice,⁵ D. Keane,⁵ J. C. Kintner,³ V. Lindenstruth,⁴ M. A. Lisa,⁶ U. Lynen,⁴ H. S. Matis,⁶ M. McMahan,⁶ C. McParland,⁶ W. F. J. Müller,⁴ D. L. Olson,⁶ M. D. Partlan,³ N. T. Porile,¹ R. Potenza,² G. Rai,⁶ J. Rasmussen,⁶ H. G. Ritter,⁶ J. Romanski,² J. L. Romero,³ G. V. Russo,² H. Sann,⁴ R. Scharenberg,¹ A. Scott,⁵ Y. Shao,⁵ B. K. Srivastava,¹ T. J. M. Symons,⁶ M. Tincknell,¹ C. Tuvé,² S. Wang,⁵ P. Warren,¹ H. H. Wieman,⁶ and K. Wolf⁷

(EOS Collaboration)

¹Purdue University, West Lafayette, Indiana 47907

²Università di Catania and Istituto Nazionale di Fisica Nucleare-Sezione di Catania, 95129 Catania, Italy

³University of California, Davis, California 95616

⁴Gesellschaft für Schwerionenforschung Darmstadt m.b.H., D-64220 Darmstadt, Germany

⁵Kent State University, Kent, Ohio 44242

⁶Nuclear Science Division, Lawrence Berkeley Laboratory, Berkeley, California 94720

⁷Texas A&M University, College Station, Texas 77843

(Received 20 May 1994)

Using reverse kinematics, we have studied the breakup of 1.0A GeV gold nuclei incident on a carbon target. The detector system permitted exclusive event reconstruction of nearly all charged reaction products. The moments of the resulting charged fragment distribution provide strong evidence that nuclear matter possesses a critical point observable in finite nuclei. We have determined values for the critical exponents γ , β , and τ . These values are close to those for liquid-gas systems and clearly different than those for 3D percolation and the liquid-gas mean field limit.

PACS numbers: 25.70.Pq, 05.70.Jk, 21.65.+f

More than a decade ago the observation of a power law distribution in the yield of intermediate mass fragments produced in high energy proton-nucleus collisions led to the suggestion that nuclear multifragmentation might be a critical phenomenon [1]. Since that time, much progress has been made in understanding how critical behavior could manifest itself in such a small system. In particular, Campi [2] suggested that the moments of the fragment distribution should exhibit features characteristic of critical phenomena if indeed intermediate mass fragments were produced in a system near its critical point. Recent experimental results from the ALADIN Collaboration [3] have shown that existing models based on nuclear physics do not describe multifragmentation data as well as a simple percolation-based model, which is known to contain critical behavior [4]. In this paper we report the results of a recent experiment conducted by the EOS Collaboration at the Lawrence Berkeley Laboratory Bevalac in which we studied the projectile fragmentation of 1.0A GeV gold nuclei incident on carbon and detected nearly all of the charged reaction products on an event-by-event basis. These exclusive data permit the first determination of the critical exponents associated with multifragmentation.

The apparatus is shown in Fig. 1. Charged particles were identified using a time projection chamber (TPC) [5] for $1 \leq Z \leq 6$, a time-of-flight wall (TOF) for $7 \leq Z \leq 10$, and a multiple sampling ionization chamber (MUSIC)

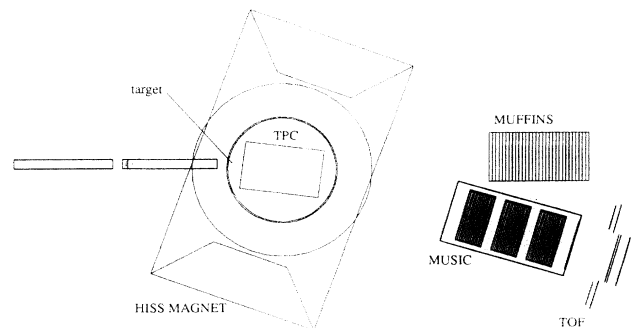


FIG. 1. The EOS experimental setup. The Muffins neutron detector was not used in this work. Beam diagnostic detectors are not shown.

[6] for $11 \leq Z \leq Z_{\text{beam}}$. Of particular importance for the analysis described below is the determination of the charged particle multiplicity and the assignment of charge to the heaviest fragments in the final state. Since most of the reaction products are below charge 6, they are detected in the TPC. Simulations show that the TPC reconstructs tracks originating from the projectile source with nearly 100% efficiency, while the efficiency for reconstructing tracks originating from the target source is low. The measurement of target tracks is not important for our analysis. The MUSIC detector has charge resolution $\sigma = 0.2e$ and was positioned such that $\sim 95\%$ of all

fragments $11 \leq Z \leq Z_{\text{beam}}$ fell within its acceptance. The TOF had a comparable acceptance. After all charged reaction products were identified, the number of fragments of each charge was determined neglecting pions. The total reconstructed charge, Z_{sum} , peaks at 79 with a full width at half maximum of 6. Only those events whose Z_{sum} was 79 ± 3 were selected for further analysis (9716 events).

For each event, we determine the multiplicity of charged fragments, m , and the number of charged fragments, n_Z , of nuclear charge Z . We then construct the k moments of this distribution:

$$M_k(m) = \sum_Z Z^k n_Z(m). \quad (1)$$

Campi [2] was the first to suggest that the *methods* developed to study large percolation lattices may be relevant to the analysis of multifragmentation data. In percolation theory the moments of the cluster distribution contain the signals for critical behavior [4]. Quantities that display divergent behavior in macroscopic systems still show a peaking behavior in finite sized systems. In fact, it is well known in percolation theory how various quantities scale with system size [7]. In the analysis described below, we have used the *methods* developed for determining percolation critical exponents to extract the critical exponents for nuclear matter from the moments of the fragment charge distributions.

We assume that m is a linear measure of the distance from the critical point [2]. We will refer to the region in m below m_c , the critical multiplicity, as the “liquid” phase and the region above m_c as the “gas” phase. Following Stauffer and Aharony [4], we omit the biggest cluster (fragment), denoted Z_{max} , from the sum of Eq. (1) when we are on the liquid side of the phase transition. Physically, Z_{max} corresponds to the bulk liquid in an infinite system. The critical exponents γ , β , and τ for large systems are given by

$$M_2 \sim |\epsilon|^{-\gamma}, \quad (2)$$

$$Z_{\text{max}} \sim |\epsilon|^\beta, \quad (3)$$

$$n_Z \sim Z^{-\tau} \quad \text{for } m = m_c, \quad (4)$$

where $\epsilon = m - m_c$ is the distance from the critical multiplicity. The exponents are not all independent [8], since

$$\tau = 2 + \frac{\beta}{\beta + \gamma}. \quad (5)$$

Equations (2)–(4) can be applied to thermal systems as well as to percolation. In a thermal system, M_2 describes the isothermal compressibility which diverges

at the critical point. In percolation it is the mean cluster size. In an infinite system Z_{max} is the order parameter of the transition. In a fluid system the order parameter is represented by the difference in density between the liquid and gas phases. This quantity is nonzero only below the critical temperature and vanishes at the critical point. Finally, Eq. (4) gives the cluster distribution at the critical point. In small systems the singular nature of Eqs. (2) and (3) is influenced by finite size effects.

We now briefly describe the procedure by which we determine the critical exponents. Further details of the method can be found in Ref. [9]. The first step is to use the second moment to determine γ . In percolation theory finite size effects can be offset by adjusting p_c from its infinite lattice value until one obtains power law behavior with the same value for γ in M_2 on both the liquid ($p < p_c$) side of the transition and on the gas side ($p > p_c$) (for bond breaking percolation). We have taken the same approach using multiplicity. We seek that value of m_c that gives the same value of γ for both the gas and liquid sides of Eq. (2). The value of γ can depend on the region of ϵ used since finite size distortions dominate as $\epsilon \rightarrow 0$, and signatures of critical behavior vanish for large ϵ , i.e., in the mean field regime.

The determination of the exponents was made by first selecting those values of m_c for which γ_{liquid} and γ_{gas} differed by no more than 10%. The distribution of m_c 's satisfying this matching criterion is peaked at 26. We have chosen $m_c = 26 \pm 1$ for our subsequent analysis. For each of these values of m_c we then make many determinations of γ , β , and τ by varying the fitting region. The value of β was determined by a fit of Eq. (3) to the liquid side. The exponent τ was determined from the slope of $\ln(M_3)$ vs $\ln(M_2)$ [2], where we have used only the gas branch of the plot. The removal of the largest fragment in the liquid branch is a major perturbation on this correlation. This feature was observed in our percolation simulations using the $L = 6$ lattice [9]. We also determined τ using Eq. (4) and obtained consistent results. Representative fits for γ and β are shown in Figs. 2 and 3, respectively. The final values for the exponents are obtained by averaging all 370 trials made for the three choices of m_c and are reported in Table I. The errors listed there are standard deviations. We note that the values of β , γ , and τ obtained using our method obey the scaling relation, Eq. (5).

The exponent values obtained via our procedure do not depend critically on our choice of a 10% slope matching criterion. Repeating our analysis requiring a more stringent 3% matching does not alter the values of the exponents. The exponent values are also relatively insensitive to m_c . Thus a change in m_c of one unit leaves the values unchanged within their statistical uncertainties. In order to judge the robustness of the exponent values with respect to Z_{sum} , we have also done the analysis for

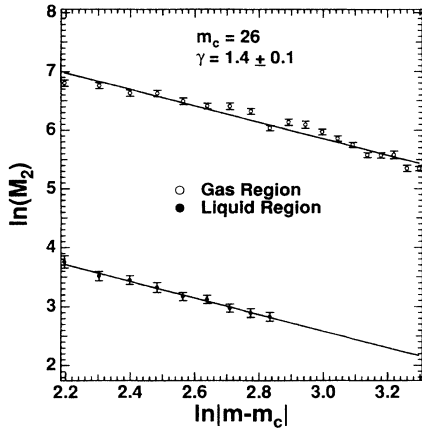


FIG. 2. Example of the determination of the critical exponent γ for particular gas and liquid fitting regions.

events with $Z_{\text{sum}} = 72\text{--}75$ or $83\text{--}86$. The results again are statistically unaltered.

Our analysis tacitly assumes that all of the projectile-related charges are associated with multifragmentation. Protons are also emitted during the prompt cascade [10] and can be evaporated from either the cascade remnant or from fragments [11]. Protons from both of these sources should in principle be excluded from the multiplicity and moments. Using a method employed at lower energies [12], we have determined that there is a linear relation between the total observed multiplicity and that associated with the post-cascade stage alone. Furthermore, the moments are dominated by the largest charges and removing protons has little effect on their value. Thus the exponents are essentially unaffected by the inclusion of cascade protons.

Our data show that the number of evaporated protons must be a small fraction of the total. Events at the critical multiplicity involve, on average, the emission

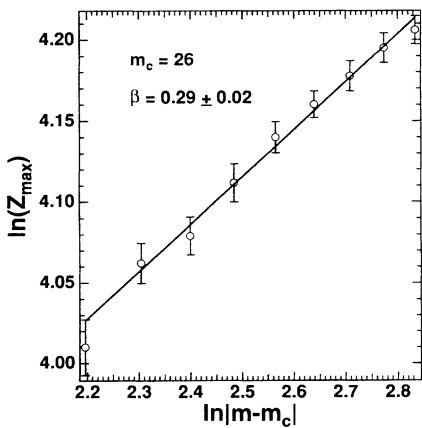


FIG. 3. Example of the determination of the critical exponent β for a particular liquid fitting region.

TABLE I. Critical multiplicity and exponents for Au projectile fragmentation and other three-dimensional systems.

Quantity	Experiment	Liquid-gas	Percolation	Liquid-gas mean field
m_c	26 ± 1			
γ	1.4 ± 0.1	1.23	1.8	1.0
β	0.29 ± 0.02	0.33	0.41	0.5
τ	2.14 ± 0.06	2.21	2.18	2.33

of 19 $Z = 1$ particles of which 11 are protons. We estimate on the basis of the proton rapidity distribution that 6 prompt protons are emitted in an event near the critical multiplicity. The power law distribution at m_c , Eq. (4), is consistent with the emission of about 10 $Z = 1$ particles in multifragmentation indicating that only 2 or 3 protons are evaporated in each critical event. Owing to the Coulomb barrier, these protons presumably come from the lighter fragments and so have a small effect on the moments.

We have selected for comparison with our data several three-dimensional systems possessing a scalar order parameter, liquid-gas [8], percolation [4], and the mean field limit of the liquid-gas system [13]. These values are also listed in Table I. When comparing the experimental exponents with the others listed in the table, we note that τ is close to 2.2 in all cases. In Fig. 4 we plot the value of β versus γ for the Au multifragmentation data and for the other systems in Table I. It is noteworthy that the fragmentation result is close to the point for liquid-gas systems and is significantly distant from either the percolation or liquid-gas mean field results. For macroscopic systems, the critical exponents describe the power law behavior of thermodynamic quantities as the critical point is approached. We expect critical behavior to be effectively

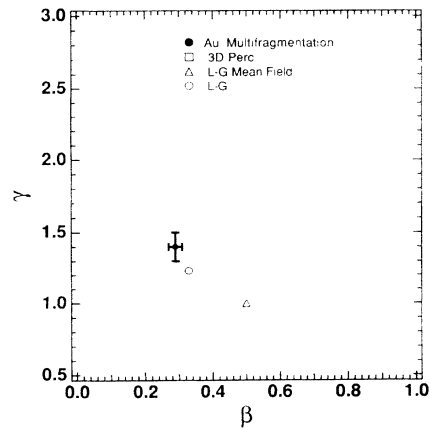


FIG. 4. γ versus β after applying selection criteria described in text. For comparison, liquid-gas, 3D percolation, and liquid-gas mean field values are shown.

observable in finite size systems as long as the characteristic length and the number of degrees of freedom are sufficiently large. We believe that the Au system achieves this based on the observed power law behavior, and thus permits the extraction of exponents which may apply to infinite nuclear matter.

In conclusion, we have analyzed the fragment distributions resulting from 1.0A GeV gold ions incident on carbon. Events in which the total reconstructed charge was within 3 units of the charge of gold were chosen for analysis. We have used techniques from percolation theory applied to small lattices [9] in order to determine independently the values of three critical exponents. The influence of finite size effects has been addressed by our procedure. The charge moments of nuclear multifragmentation provide strong evidence for critical behavior in finite nuclei. We find that these exponents are close to the nominal liquid-gas values. A number of open questions remain, most importantly whether the system is in thermal equilibrium and, if so, whether the multiplicity is proportional to temperature. To answer these questions and to further characterize this phenomenon, work is in progress to understand the dynamics of the multifragmentation process.

This work was supported in part by the U.S. Department of Energy under Contracts or Grants No. DE-AC03-76SF00098, No. DE-FG02-89ER40531,

No. DE-FG02-88ER40408, No. DE-FG02-88ER40412, No. DE-FG05-88ER40437, and by the U.S. National Science Foundation under Grant No. PHY-91-23301.

*Current address: Sung Kwun Kwan University, Suwon 440-746, Republic of Korea.

- [1] J. E. Finn *et al.*, Phys. Rev. Lett. **49**, 1321 (1982); R. W. Minich *et al.*, Phys. Lett. **118B**, 458 (1982).
- [2] X. Campi, J. Phys. A **19**, L917 (1986); Phys. Lett. B **208**, 351 (1988).
- [3] P. Kreuz *et al.*, Nucl. Phys. **A556**, 672 (1993).
- [4] D. Stauffer and A. Aharony, *Introduction to Percolation Theory* (Taylor and Francis, London, 1992), 2nd ed.
- [5] G. Rai *et al.*, IEEE Trans. Nucl. Sci. **37**, 56 (1990).
- [6] W. Christie *et al.*, Nucl. Instrum. Methods Phys. Res., Sect. A **255**, 46 (1987).
- [7] D. Stauffer, Phys. Rep. **54**, 1 (1979).
- [8] H. E. Stanley, *Introduction to Phase Transitions and Critical Phenomena* (Oxford University Press, Oxford, 1971).
- [9] J. B. Elliott *et al.*, Phys. Rev. C **49**, 3185 (1994).
- [10] Y. Yariv and Z. Fraenkel, Phys. Rev. C **20**, 2227 (1979).
- [11] R. J. Charity *et al.*, Nucl. Phys. **A483**, 371 (1988).
- [12] D. Cussol *et al.*, Nucl. Phys. **A561**, 298 (1993).
- [13] H. B. Callen, *Thermodynamics and an Introduction to Thermostatistics* (John Wiley and Sons, New York, 1985), 2nd ed.

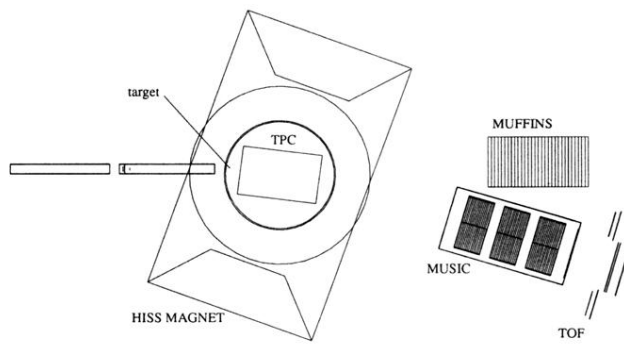


FIG. 1. The EOS experimental setup. The Muffins neutron detector was not used in this work. Beam diagnostic detectors are not shown.